ACCOUNTS of chemical research

Article

Cite This: Acc. Chem. Res. 2017, 50, 2440-2448

pubs.acs.org/accounts

Supramolecular Assembly of Peptide Amphiphiles

Published as part of the Accounts of Chemical Research special issue "Chemical Biology of Peptides".

Mark P. Hendricks,[†] Kohei Sato,[†] Liam C. Palmer,[†,‡] and Samuel I. Stupp*[,†,‡,§,∥,⊥]

[†]Simpson Querrey Institute for BioNanotechnology, Northwestern University, Chicago, Illinois 60611, United States

[‡]Department of Chemistry, Northwestern University, Evanston, Illinois 60208, United States

[§]Department of Materials Science and Engineering, Northwestern University, Evanston, Illinois 60208, United States

[∥]Department of Medicine, Northwestern University, Chicago, Illinois 60611, United States

[⊥]Department of Biomedical Engineering, Northwestern University, Evanston, Illinois 60208, United States

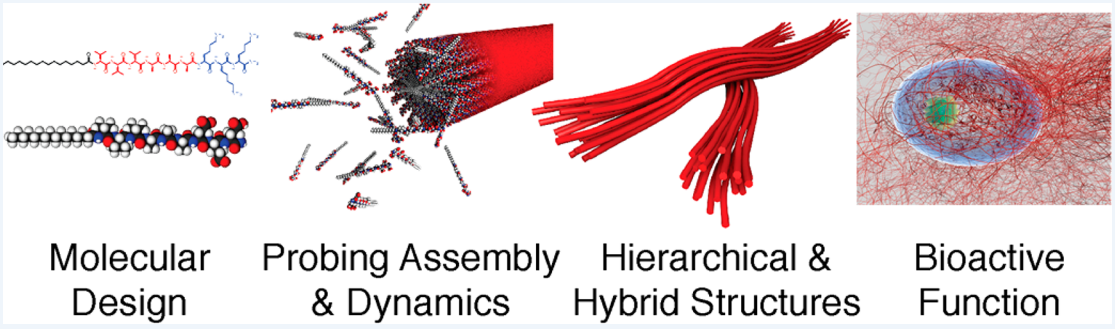

CONSPECTUS: Peptide amphiphiles (PAs) are small molecules that contain hydrophobic components covalently conjugated to peptides. In this Account, we describe recent advances involving PAs that consist of a short peptide sequence linked to an aliphatic tail. The peptide sequence can be designed to form β-sheets among the amino acids near the alkyl tail, while the residues farthest from the tail are charged to promote solubility and in some cases contain a bioactive sequence. In water, β-sheet formation and hydrophobic collapse of the aliphatic tails induce assembly of the molecules into supramolecular one-dimensional nanostructures, commonly high-aspect-ratio cylindrical or ribbonlike nanofibers. These nanostructures hold significant promise for biomedical functions due to their ability to display a high density of biological signals on their surface for targeting or to activate pathways, as well as for biocompatibility and biodegradable nature.

Recent studies have shown that supramolecular systems, such as PAs, often become kinetically trapped in local minima along their self-assembly reaction coordinate, not unlike the pathways associated with protein folding. Furthermore, the assembly pathway can influence the shape, internal structure, and dimension of nanostructures and thereby affect their bioactivity. We discuss methods to map the energy landscape of a PA structure as a function of thermal energy and ionic strength and vary these parameters to convert between kinetically trapped and thermodynamically favorable states. We also demonstrate that the pathway-dependent morphology of the PA assembly can determine biological cell adhesion and survival rates.

The dynamics associated with the nanostructures are also critical to their function, and techniques are now available to probe the internal dynamics of these nanostructures. For example, by conjugating radical electron spin labels to PAs, electron paramagnetic resonance spectroscopy can be used to study the rotational diffusion rates within the fiber, showing a liquidlike to solidlike transition through the cross section of the nanofiber. PAs can also be labeled with fluorescent dyes, allowing the use of super-resolution microscopy techniques to study the molecular exchange dynamics between PA fibers. For a weak hydrogen-bonding PA, individual PA molecules or clusters exchange between fibers in time scales as short as minutes. The amount of hydrogen bonding within PAs that dictates the dynamics also plays an important role in biological function. In one case, weak hydrogen bonding within a PA resulted in cell death through disruption of lipid membranes, while in another example reduced hydrogen bonding enhanced growth factor signaling by increasing lipid raft mobility.

PAs are a promising platform for designing advanced hybrid materials. We discuss a covalent polymer with a rigid aromatic imine backbone and alkylated peptide side chains that simultaneously polymerizes and interacts with a supramolecular PA structure with identical chemistry to that of the side chains. The covalent polymerization can be "catalyzed" by noncovalent polymerization of supramolecular monomers, taking advantage of the dynamic nature of supramolecular assemblies. These novel hybrid structures have potential in self-repairing materials and as reusable scaffolds for delivery of drugs or other chemicals. Finally, we highlight recent biomedical applications of PAs and related structures, ranging from bone regeneration to decreasing blood loss during internal bleeding.

Received: June 13, 2017
Published: September 6, 2017

DOI: 10.1021/acs.accounts.7b00297
Acc. Chem. Res. 2017, 50, 2440−2448

INTRODUCTION

Peptide supramolecular assemblies can compete with designed proteins in their capacity to offer useful biological functions and structural diversity to synthetic soft matter. This potential is particularly interesting given the possibility of integrating multiple biological functionalities into a supramolecular scaffold of peptides. From a structural perspective, peptide assemblies can generate filaments, 2D-sheets, spheres, networks, tubes, helices, and more complex shapes that will no doubt be discovered in the future as we learn to master morphogenesis of peptide assemblies. This Account focuses on a peptide amphiphiles (PAs), an important family of peptides with enormous potential to create biological functionality and structure. These molecules are peptides modified with hydrophobic segments, such as lipid tails, at their termini or at specific residues in the sequence.

Early reports on the synthesis of lipidated peptides used solution reactions,[1,2] and subsequently Tirrell and co-workers reported the use of a more efficient method using solid-phase synthesis. Previous work on lipidated peptides was motivated by interest in the use of molecules to investigate bioactivity in environments that mimic cell membranes,[3] and also by their role in eukaryotic cells.[4] In 2001 the Stupp laboratory reported the first example of PA molecules that self-assembled into long nanofibers with the capacity to form hydrogel biomaterials and mimic the extracellular matrix.[5] These nanofibers could display biological signals on their surfaces, and hydrogel formation could be driven by a decrease in charge density on the amino acid residues.[5] Additionally, these first supramolecular PA nanofibers were designed to nucleate apatite crystals on their surfaces with specific crystallographic orientation relative to the fiber axis, mimicking the nanoscale structure of bone, and to enable covalent capture of the supramolecular assemblies through oxidative coupling of cysteine residues in the peptide sequence. Since the first report in 2001, the Stupp laboratory has continued to study PAs. Typical fiber-forming PA molecules from our laboratory consist of a peptide sequence, often containing fewer than 10 amino acids, linked to an aliphatic tail with more than 10 carbon atoms (Figure 1, center). The peptide sequence contains a domain adjacent to the alkyl tail with a high propensity to form β-sheets, followed by charged residues to promote solubility in water, and in some cases ending with spacers for molecular flexibility linked to a bioactive component. In water, hydrophobic collapse of the aliphatic tails and formation of hydrogen bonds among the peptide segments leads to the formation of "filamentous" assemblies, often with a high aspect ratio owing to the β-sheet domain. These assemblies can be structured as cylinders, ribbons, twisted structures, or aggregates of more than one fiber, among others (see Figure 1).[6] We have extensively studied how the molecular structure of the PA molecules, especially the peptide sequence and the alkyl tail, influence the β-sheet character, morphology, surface chemistry, and potential bioactivity of the resulting nanostructures.[7,8] We have also investigated various methods to induce assembly, including concentration, pH, and the presence of divalent ions.[7,8]

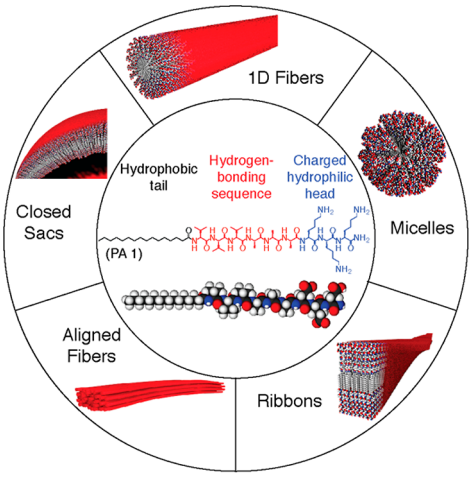

Figure 1. General structure of a PA (center) surrounded by many of the supramolecular nanostructures that have been formed from this system.

Our group has had a longstanding interest in PAs as functional materials, especially for regenerative medicine and cancer therapy, owing to their ability to interact with cells through a high density of surface signals and mimic the extracellular matrix.[9] We have included bioactive epitopes on the nanofiber surface and shown them to have tumoricidal activity. For example, we discovered a nanostructure that induced breast cancer cell death by caspase-independent and Bax/Bak-independent mechanisms associated with membrane disruption, inducing cell death more robustly in transformed breast epithelial cells than in untransformed cells, suggesting a degree of tumor selectivity.[10] Using an orthotopic mouse xenograft model of breast cancer, systemic administration of different cytotoxic nanostructures significantly reduced tumor cell proliferation and overall tumor growth, demonstrating the potential of multifunctional PA nanostructures as versatile cancer therapeutics.[11] Another method in which PAs can affect tumors is through pH-dependent structural changes, which we have shown can influence drug encapsulation and tumor accumulation.[12] PAs have also shown potential to induce rapid differentiation of progenitor cells into neurons, while suppressing the development of astrocytes, by encapsulating neural progenitor cells within a three-dimensional network of PA nanofibers that present the neurite-promoting laminin epitope IKVAV.[13] Additionally, PA nanofibers have demonstrated potential as a therapy for ischemic cardiovascular disease by mimicking the activity of VEGF, one of the most potent angiogenic signaling proteins.[14] By presenting VEGF-mimetic peptide sequences on the surface of the nanostructure, these structures induce phosphorylation of VEGF receptors and promote proangiogenic behavior in endothelial cells, and elicit an angiogenic response in the host vasculature in a chicken embryo assay. When evaluated in a mouse hind-limb ischemia model, the nanofibers increased tissue perfusion, functional recovery, limb salvage, and treadmill endurance compared to controls.

Beyond their assembly into nanofibers and related nanostructures, we have investigated the hierarchical assembly of PAs into macroscale configurations. One example is their assembly into macroscopic sacs and membranes at the interface between two aqueous solutions, one containing a PA and the other containing a high molecular weight polymer of opposite charge. The resulting structures have a highly ordered architecture in which a diffusion barrier forms almost instantaneously, followed by diffusion of the polymer into the PA solution, driven by a dynamic synergy between osmotic pressure of ions and static self-assembly, which results in fibrils that grow perpendicular to the membrane.[15,16] Additionally, we have shown that long PA fibers can be aligned over macroscopic scales by annealing and manually dragging the resulting liquid crystal from a pipet into salty media, which can create monodomain viscoelastic strings over centimeters long.[17] Unsurprisingly, these noodle-shaped viscoelastic strings are highly bioactive;[17] for example, they can provide direction and promote

DOI: 10.1021/acs.accounts.7b00297
Acc. Chem. Res. 2017, 50, 2440−2448

the growth of neurites from neurons when formed with epitope-displaying PAs.[18]

SELF-ASSEMBLY PATHWAYS

An emerging theme in supramolecular systems is the importance of self-assembly pathways. While the assembly pathways of proteins are well-known to be critical to their correct folding and function, the analogous question regarding supramolecular systems—even those employing peptides—has not been widely explored. When supramolecular systems are designed, dominant interactions are typically targeted that would drive assembly under thermodynamic conditions. However, it has become apparent that these systems, like the more complicated proteins, frequently become kinetically trapped in local minima along the reaction coordinate. Moreover, the optimal function of supramolecular systems can be associated with kinetically trapped states and out-of-equilibrium systems, which may be interesting as "active matter" by dissipating energy from external stimuli.

Since controlling the structure of peptide amphiphile assemblies is critical for their function, investigating the pathways through which they assemble has become a topic of great interest. The first example of this effort, by Meijer and Stupp, utilized solvents that either solubilize the monomer (hexafluoroisopropanol, HFIP) or induce assembly (water).[19] It was observed that the assembly pathway of $C_{16}V_3A_3E_3$ can determine the supramolecular morphology and assembly rate, with increasing HFIP concentration resulting in smaller aggregates that exhibit less β-sheet character and slower assembly kinetics. A volume ratio of 21% HFIP in water was the critical fraction that induced spontaneous nucleation of β-sheet-containing fibers, and these fibers were kinetically stable and did not disassemble upon addition of HFIP at room temperature. The Stupp laboratory has since sought to more fully measure and navigate the energy landscape of PA assembly in order to direct their architecture.[20] We explored the landscape of a PA with the sequence $V_3A_3K_3$ conjugated to a C_{16} alkyl chain at the N-terminus (PA **1**, Figure 1).[20] The main intermolecular forces that affect this structure are electrostatic repulsion between the positively charged lysine residues and hydrogen bonding among the β-sheet V_3A_3 sequence. The strength of electrostatic repulsion can be reduced by increasing the ionic strength of the solution to screen the interactions between lysine residues, thus favoring β-sheet formation.

It was observed that the PA fibers behaved differently when a critical ionic strength (I_c) of 6 mM was reached, independent of whether the ionic strength was caused by the PAs themselves or added salt. This is most clear in the thermodynamic states obtained by annealing a PA solution: below the I_c, fairly monodisperse fibers of about 150 nm in length form, whereas above the I_c only exceptionally long fibers are visible (Figure 2a left and right, respectively). Once annealed, these solutions can be perturbed away from their thermodynamic condition by adjusting the ionic strength through the addition of salt or dilution, which results in a change in the β-sheet character (Figure 2b) but little immediate change to the fiber structure. However, both fibers eventually revert back to the thermodynamic state. The short fibers grew into the thermodynamically favored long fibers over days at room temperature, suggesting a metastable state with a

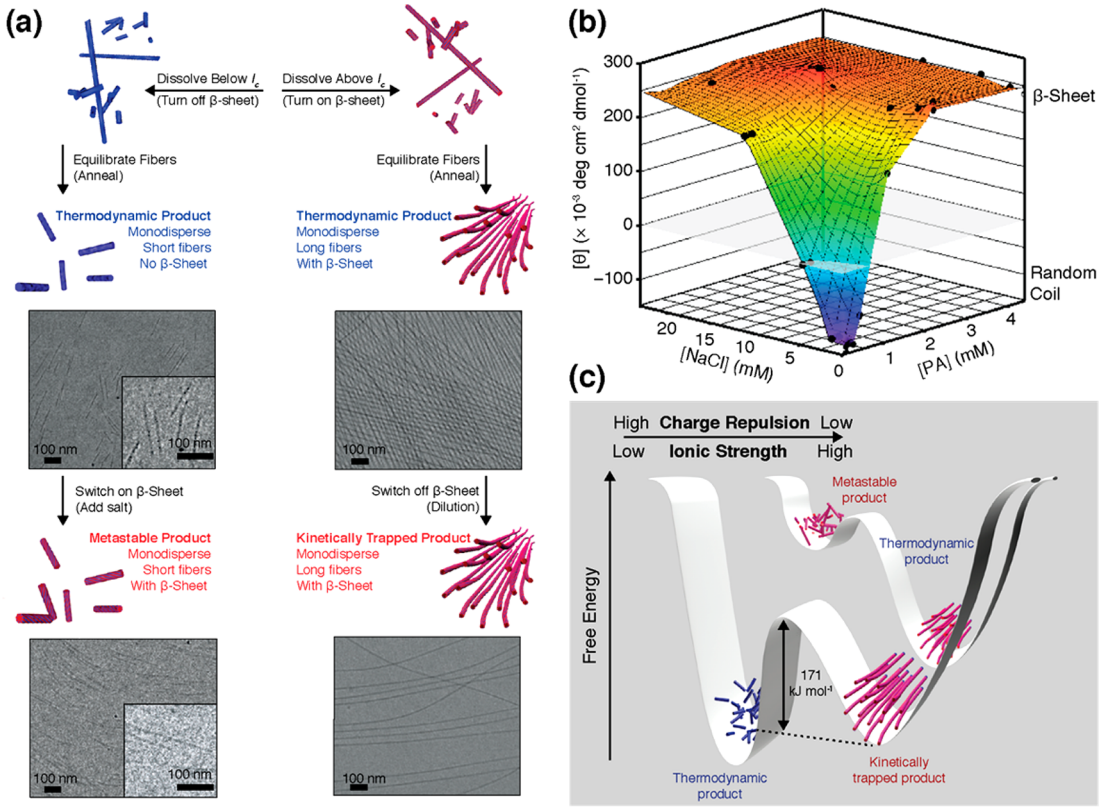

Figure 2. (a) Schematics and representative cryo-TEM micrographs of structures obtained following assembly pathways initially below (left) and above (right) the I_c by first annealing to form the thermodynamically favored product, and then adding salt (left) or diluting (right) to obtain the nonthermodynamic structures. (b) Map of CD signal at 202 nm plotted as a function of PA and salt concentrations. (c) Schematic representation of the free energy landscapes of PA assemblies below and above the critical ionic strength (front and back, respectively). Adapted with permission from ref 20. Copyright 2016 Nature Publishing Group.

DOI: 10.1021/acs.accounts.7b00297
Acc. Chem. Res. 2017, 50, 2440−2448

low barrier to conversion, whereas the long fibers were stable at room temperature for days but converted to the short fibers upon heating, suggesting a kinetically trapped state with an intermediate barrier to conversion (estimated at 170 kJ mol^{-1} using an Arrhenius plot). Together, these results allowed us to define two distinct energy landscapes dependent on the ionic strength of the solution, as shown in Figure 2c.

To explore the connection between the structure and function of these systems and their energy landscape, we studied how cells react to the structures obtained through the pathways described above. The thermodynamically favored long fibers promoted biological cell adhesion and survival, whereas the metastable product, characterized by short fibers, interferes with adhesion and can lead to cell death. Moving forward there is significant opportunity to develop functional supramolecular systems in which molecular building blocks can be controllably assembled into numerous supramolecular structures depending on the pathway followed.

DYNAMICS

Our interest in understanding the energy landscapes of peptide amphiphiles and the possible pathways between the assembled nanostructures naturally led us to explore the dynamics of these systems at the molecular level. Until recently experimental techniques have not been available that provide high spatial and temporal resolution on dynamics, thus limiting our knowledge of these processes to insights obtained through simulations. To better understand the intrinsic dynamics of PA assemblies, we undertook a quantitative study of the conformational dynamics of PAs **2** and **3**, in which PA **3** has a *N*-methylated valine to reduce the hydrogen bonding within its assembled fibers (Figure 3a).[21] Electron paramagnetic resonance (EPR) spectroscopy was used to investigate the PA molecular dynamics by incorporating small nitroxyl radical electron spin labels at specific sites (PAs **4**−**8**). By carrying out quantitative EPR on nanofibers coassembled with 0.4% of the spin-labeled PA, rotational diffusion rates were determined at the labeled sites which allowed a measure of the internal dynamics. The internal structure changed from liquidlike to solidlike through the cross section of the supramolecular PA nanofiber, with solidlike behavior concentrated in the interior of the nanostructures near the highest densities of hydrogen bonds in β-sheet structures (Figure 3b). Unsurprisingly, nanofibers that included PA **3** were more dynamic, which can be attributed to the reduced hydrogen bonding in these structures.

In addition to the internal molecular dynamics discussed above, there is also interest in understanding the dynamics of molecular exchange between PA nanostructures. This led us to explore the use of super-resolution microscopy techniques, which provide powerful tools to reveal the spatial distribution of molecules at the nanoscale. For example, stochastic optical reconstruction microscopy (STORM) can realize resolutions on the order of tens of nanometers, which is an order of magnitude below the diffraction limit of visible light and approaching the molecular scale. The resolution improvement is accomplished by repeatedly exciting a small proportion of fluorescent molecules associated with the sample, accurately mapping the individual fluorophores, and reconstructing an image by overlaying the resulting localizations. Thus far, these techniques have primarily been utilized for imaging fine details of cellular structures, but we suspected that the ability of STORM to image individual nanofibers and the molecular distributions within them would make it a powerful tool to study the molecular exchange of peptide amphiphile nanofibers. To do so, water-soluble sulfonated dyes

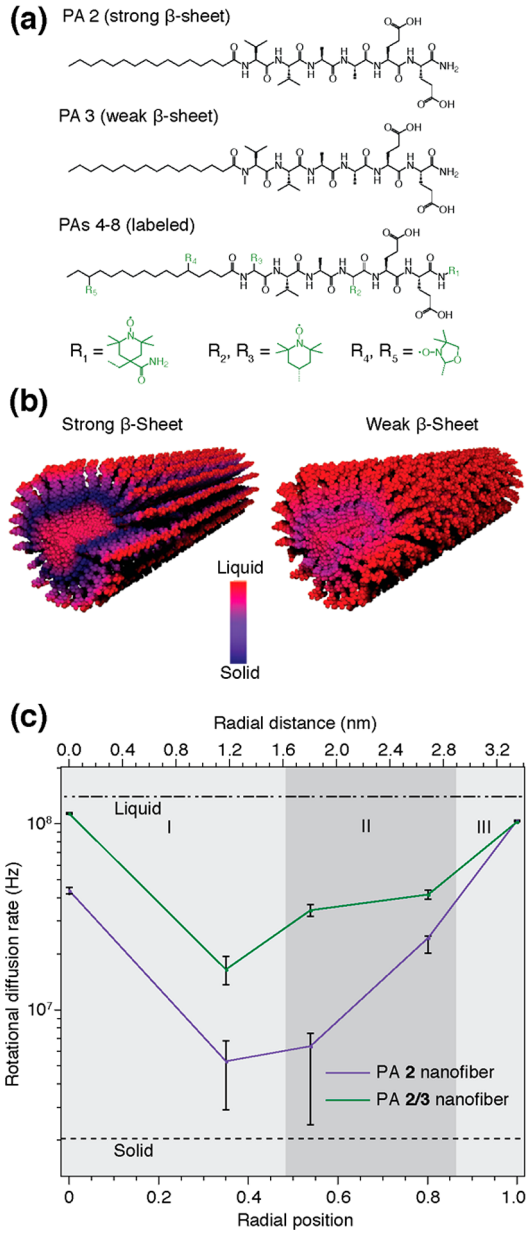

Figure 3. (a) Chemical structures of the PA molecules investigated. Note that PA **3** contains an *N*-methylated valine to reduce intermolecular hydrogen bonding. PAs **4**−**8** are labeled with radical-electron spin labels, each with a single radical at the position highlighted and the chemical structure shown below. (b) Heat map of the liquid vs solid-life character of nanofibers composed of PA **2** (left) and PA **2**/**3** (right). The vertical bar indicates the gradient of solidlike to liquidlike dynamics (blue and red, respectively) through the nanofiber cross sections. (c) Rotational diffusion rates (k_r) extracted from EPR spectral with each spin in the nanofiber, plotted against theoretical radial position. Reproduced with permission from ref 21. Copyright 2014 Nature Publishing Group.

(Cy3, green; Cy5, red) were conjugated to PAs consisting of a C_{16}-tail, six alanines in the β-sheet forming region, and three glutamic acids to promote solubility as shown in Figure 4a.[22] Alanine has a weaker propensity to form β-sheets than valine, so using this amino acid in the β-sheet forming segment was anticipated to result in relatively dynamic PA nanostructures. To measure the exchange of PA molecules between fibers, two sets of single-color PA nanofibers were separately preassembled

DOI: 10.1021/acs.accounts.7b00297
Acc. Chem. Res. 2017, 50, 2440−2448

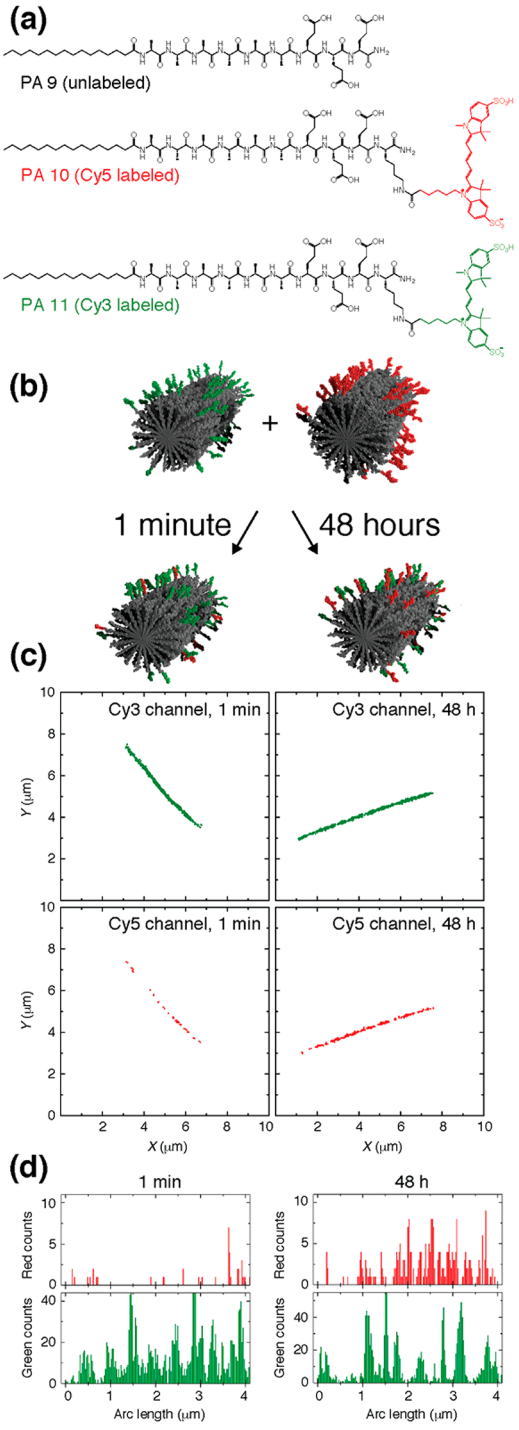

Figure 4. (a) Chemical structures of PAs **9**-**11**. (b) Schematic of a molecular exchange kinetic measurement. (c) Localization maps of PA nanofibers immobilized on a glass coverslip at different time points, after applying necessary corrections. (d) Histograms depicting the localization density profiles along the nanofiber backbone. Reproduced with permission from ref 22. Copyright 2016 Nature Publishing Group.

in aqueous buffer by mixing 5% of either PA **10** or **11** into PA **9**, followed by aging at room temperature for 16 h. The two aged solutions were brought to 37 °C and mixed, allowing for molecular exchange, as represented in Figure 4b. Two-color STORM images were then acquired of aliquots removed from the solution at different time points over 48 h. Figure 4c shows representative PA nanofibers 1 min and 48 h after mixing. As clearly revealed in these images, the fibers initially containing a single label partially mix after only 1 min, and are completely mixed after 48 h.

The distribution of dyes inserting into initially single-color nanofibers was quantified using correlative image analysis. The results are consistent with an exchange mechanism in which monomers or small clusters of molecules insert randomly into a fiber, based on the histograms that show variable localization densities along the nanofiber backbone (Figure 4d). Different exchange rates are observed within the same fiber, implying that areas of local cohesiveness exist that are perhaps caused by β-sheet discontinuous domains. The results show that these supramolecular systems are highly dynamic and that the intermolecular interactions affect their exchange mechanisms. The fundamental significance of this observation is that strong interactions within supramolecular nanostructures, like strong β-sheet hydrogen bonding, lead to exchange of clustered molecules, thus generating a large diversity of structures. This is in contrast to supramolecular nanostructures with weak intermolecular interactions, such as typical lipid spherical or wormlike micelles, where exchange occurs completely at the monomeric scale and any supramolecular structures are fairly homogeneous. This has implications for future strategies to search supramolecular libraries for systems with optimal functions, including capacity to bind specific molecules or even catalytic activity.

Building on the growing understanding of PA dynamics, there was a desire to further probe the impact of their internal dynamics on cells. Although the effects of hydrophobicity and cationic charge of soluble molecules on the cell membrane are well-known, the interactions between materials with these molecular features and cells remain poorly understood. To study these material−cell interactions, the forces were varied within nanofibers of PAs and it was found that this significantly impacts cell survival rates.[23] PA **12** forms fibers similar to those previously described, but demonstrated strong cytotoxicity and rapid cell death and thus provided a foundation to design molecules that improved cellular interactions (Figure 5a). The cationic charge and hydrophobic tail were required for cell toxicity, as both the peptide sequence itself and anionic analogue of PA **12** were found to be nontoxic. The nontoxic nature of the anionic PA is perhaps due to electrostatic repulsion, as the cell surface is negatively charged due to the presence of glycoproteins and polysaccharide chains. Furthermore, reducing the amphiphilicity of the assembling molecules by either decreasing the alkyl tail length from 16 to 12 carbons or removing one lysine residue resulted in cell viability.

Although hydrophobicity and cationic charge influence the cytotoxicity of PA assemblies, the most striking difference was observed when modifying β-sheet hydrogen bonding among molecules within the nanostructure. PA **12** contains glycine residues and therefore has a relatively weak ability to hydrogen bond, whereas PA **13** contains valine residues, which have a higher propensity for strong β-sheet hydrogen bonding. Interestingly, cell toxicity diminished when cells were exposed to PA **13** nanofiber coatings as indicated by viability staining (Figure 5b) and the lack of cytoplasmic enzyme lactate dehydrogenase release. These patterns in cell toxicity were observed across multiple cell types, including MC3T3-E1 preosteoblasts, MB-MDA-231 breast cancer cells, and primary human mesenchymal stem cells (hMSCs). We hypothesized that the cause of the toxicity of PA **12** may be an interaction with the cell membrane, which led us to study its interaction with

DOI: 10.1021/acs.accounts.7b00297
Acc. Chem. Res. 2017, 50, 2440−2448

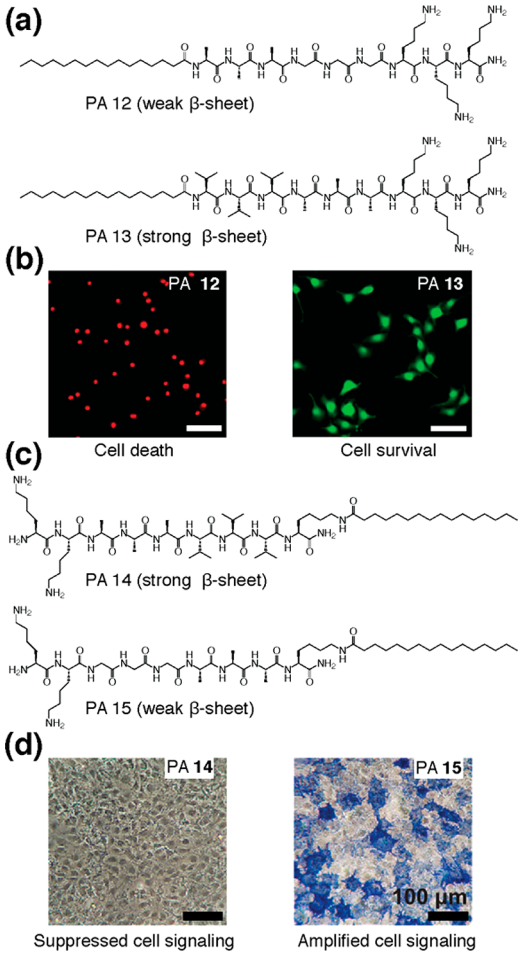

Figure 5. (a,c) Chemical structures of PAs **12**−**15** that vary the propensity for intermolecular hydrogen bonding adjacent to the tail. (b) Representative fluorescence images of MC3T3-E1 cells that are viable (green, calcein) or dead (red, EthD-1) on coatings of each PA after 4 h of culture. Scale bars, 100 μm. (d) Fast Blue staining to visualize alkaline phosphatase activity after 3 days of culture. Reproduced with permission from refs 23 (a,b) and 24 (c,d). Copyright 2014 Nature Publishing Group (a,b) and 2016 American Chemical Society (c,d).

liposomes. Liposomes made of egg phosphatidylcholine were unchanged in the presence of PA **13**, but PA **12** destroyed the liposomes within a few minutes. Cryo-transmission electron microscopy (TEM) and differential scanning calorimetry of PAs with liposomes of dipalmitoyl-phosphatidylcholine showed PA **12** significantly perturbed the liposomes from their normal state, while PA **13** minimally changed their behavior. We concluded that weak intermolecular bonds promote cell death through disruption of lipid membranes, while materials reinforced by hydrogen bonds enable cell viability, thus providing insight for new strategies to design biomaterials that interact with the cell membrane.

Knowing that weak cohesive forces within a PA fiber can result in interactions with membranes, we sought to understand the influence that this phenomenon would have on signaling pathways and thus combined PAs with low concentrations of osteogenic growth factor.[24] In this case, PA **15**, which has weaker internal hydrogen bonding due to the presence of glycine, resulted in enhanced BMP-2 and Wnt mediated signaling in myoblasts and osteogenic growth factor, respectively. Alternatively, PA **14**, with a strong propensity for hydrogen bonding, caused a reduction in BMP-2 signaling. This is clearly shown in Figure 5d, in which the alkaline phosphatase activity was much higher in the presence of PA **15** compared with PA **14**. We hypothesized that this is related to the ability for the PAs with weaker internal hydrogen bonding to increase diffusion within membrane lipid rafts, which was observed in the fluorescence recovery after photobleaching in live C2C12 cells. This work suggests that PAs and other nanostructures that can interact with cell membranes may provide a route to influence growth factor signaling.

COVALENT−NONCOVALENT HYBRID POLYMERIZATION

In addition to their use as a platform for studying supramolecular assembly, PAs have been used as a platform for developing advanced hybrid materials. We recently developed a polymeric system based on the first example of simultaneous covalent and noncovalent polymerization. The monomers used for covalent and supramolecular polymerization contained structurally matched peptide amphiphile segments.[25] An aromatic dialdehyde (monomer **16**) and aromatic diamine (monomer **17**) were conjugated to the VEVE sequence via a C_{12}-alkyl linker (Figure 6a). These two monomers are capable of forming imine bonds via a condensation reaction to polymerize covalently. When monomers **16** and **17** were mixed in a 1:1 ratio in aqueous solution at pH 5 to promote the condensation reaction, heterogeneous one-dimensional nanostructures were formed. The covalent polymer adopts a C_6-helicoidal conformation stabilized by hydrogen bonds among the peptide segments, as well as π-π stacking interactions between aromatic groups (Figure 6b). Monomer **18** is a PA that is isostructural with the side chains of monomers **16** and **17** (Figure 6a), which can form ribbon-shaped supramolecular polymers as reported previously (Figure 6c).[26] However, when monomers **16**−**18** were mixed simultaneously in a molar ratio of 1:1:2, one-dimensional structures with a well-defined cylindrical shape formed, rather than the flat assemblies of the supramolecular polymer (Figure 6d,e).

The supramolecular component (monomer **18**) in these hybrid structures can be removed by dilution and dialysis, resulting in short fibers. Addition of fresh monomer **18** to the extracted sample reconstituted the long cylindrical morphology of the covalent-noncovalent hybrid, implying that the structure can regenerate itself. (Figure 7a,b). The mechanism of the formation of the hybrid polymer was studied by circular dichroism (CD) spectroscopy, wherein the covalent-noncovalent polymer formed by mixing all three monomers simultaneously exhibited a faster increase in ellipticity than the components on their own, suggesting nucleation and growth involving simultaneous supramolecular and covalent polymerizations (Figure 7c). The average molecular weight of the covalent-only polymer made of **16** and **17** was on the order of 14 kDa, but a much higher molecular weight of 250 kDa was measured for the covalent component of the covalent-noncovalent hybrid structure. This result supports the notion that formation of the supramolecular compartment in the hybrid effectively "catalyzes" covalent polymerization, which can perhaps be viewed as a rudimentary analog of how covalent peptide synthesis is "catalyzed" by ribosomes in vivo (Figure 7d). In the ribosomal synthesis of proteins, covalent bonds among the amino acids occur in a highly structured supramolecular environment which not only templates the sequence of monomers,

DOI: 10.1021/acs.accounts.7b00297
Acc. Chem. Res. 2017, 50, 2440−2448

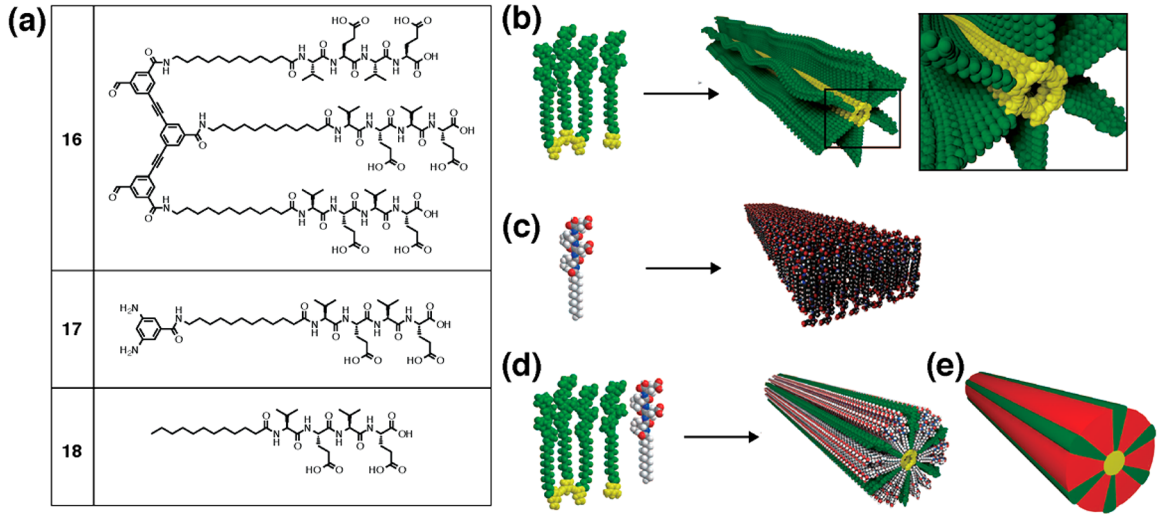

Figure 6. (a) Chemical structures of monomers **16**−**18**. Molecular graphics illustrations of (b) the covalent polymerization of monomers **16** and **17**, (c) the supramolecular polymerization of monomer **18**, and (d) the simultaneous covalent and supramolecular polymerizations that yield the hybrid polymer. (e) Schematic representation of the covalent-noncovalent hybrid polymer consisting of two distinct covalent (green and yellow) and supramolecular (red) compartments. Reproduced with permission from ref 25. Copyright 2016 American Association for Advancement of Science.

but must also contribute to favorable thermodynamics for efficient chain formation.

RECENT BIOMEDICAL APPLICATIONS OF PAs AND PEPTIDE-HYBRIDS

As previously mentioned, a key characteristic of PAs is their ability to display bioactive signals on their surface, which our group has exploited for many biomedical applications.[13,14,18] Adding to this, we recently conjugated a trisulfated monosaccharide to a PA using a flexible linker to mimic heparin sulfate.[27] The resulting nanofibers are able to bind five critical growth-factor proteins with different polysaccharide binding domains while maintaining their structure. These fibers dramatically increased signaling of bone morphogenetic protein 2 compared with natural heparin, and prompted bone regeneration in a rat posterolateral lumbar intertransverse spinal fusion model at doses 100-fold less than normally required.

In the implementation above and most other regenerative and oncological applications as highlighted in the Introduction, PAs are traditionally surgically localized in specific tissues for their application. More recently our group has initiated research on the use of PA nanostructures for intravenous systemic delivery containing molecular information to target therapies to specific sites of the body. For example, a targeted nanotherapy was designed for the treatment of noncompressible torso hemorrhage (i.e., bleeding that cannot be stopped by external compression), which is a leading cause of mortality in major trauma.[28] One tissue-factor binding sequence was found that reduced the overall blood loss in a punch biopsy-induced liver hemorrhage in vivo by 60% versus sham ($p < 0.05$) when covalently incorporated onto the nanofiber surface while maintaining biocompatibility.[28]

In addition to our laboratory's work on PAs, we are interested in other peptide-hybrid structures with biomedical functions, such as neural stem cell differentiation. Inspired by the design of DNA nanotubes reported previously,[29] we developed a DNA-based nanotube conjugated to the cell-adhesion peptide arginine-glycine-glutamic acid-serine (RGDS).[30] The RGDS peptide was attached to the s1a strand, resulting in nanotubes presenting a single peptide per tile with a periodicity of 14 nm along the tile axis and 4 nm around its circumference. Compared to the uncoated surface and nontube forming DNA−peptide aggregates, neural stem cells showed preferential differentiation into neurons rather than astrocytes with the DNA-peptide nanotubes. The nanotube morphology and chemical signals may be synergistically responsible for the selective differentiation, with the regularly controlled spacing between RGDS signals perhaps also playing a role.

CONCLUSION/OUTLOOK

Expanding the potential of supramolecular peptide nanostructures for biomedical functions will benefit from many exciting new areas under development in chemistry and materials science. Among these is supramolecular dynamics within nanostructures, especially dynamics that can react to biological environments, causing a reconfiguration that changes or optimizes their function. There is certainly much more coming in the area of dynamics in future years. Another direction is to learn how to master precise spatial positioning of multiple signals within a peptide nanostructure. This area will advance as better imaging techniques are developed, and a deeper understanding of intermolecular interactions is achieved. A third direction is to enhance the power of synthetic chemistry by integrating it with the potent biological functions of peptide nanostructures and their self-assembly potential provided by billions of years of evolution. Potential areas of chemistry that could be effectively integrated into hybrid nanomaterials include synthetic macromolecules, nucleic acids, glycans, and nanoscale inorganics.

This Account highlights the potential of supramolecular peptide nanotechnology in biomedical therapies that are very much on the horizon. Additionally, our intent was to convey the great scientific opportunity in using peptide assemblies to learn about supramolecular dynamics and the complex energy landscapes of large collections of molecules, particularly as they relate to useful functions. This will allow us to take full advantage

DOI: 10.1021/acs.accounts.7b00297
Acc. Chem. Res. 2017, 50, 2440−2448

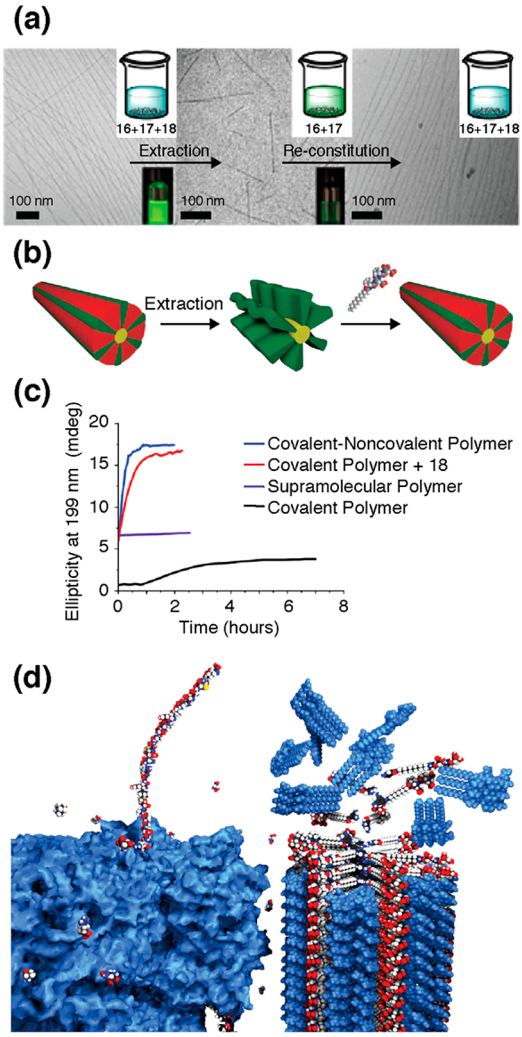

Figure 7. (a) Cryo-TEM images and (b) schematic of the covalent−noncovalent hybrid polymer (left), the same material after extraction of the supramolecular compartments by dialysis (middle), and after reconstitution of the hybrid by adding a fresh solution of monomer **18** (right). (c) Change in ellipticity at 199 nm as a function of time during formation of the covalent-polymer, supramolecular-polymer, and covalent-noncovalent hybrid polymer during simultaneous covalent and supramolecular polymerization (by mixing monomers **16**−**18**), as well as the covalent-noncovalent hybrid polymer by adding monomer **18** to a preformed covalent-polymer. (d) Schematic showing ribosomal synthesis of peptides (left) and simultaneous hybrid polymerization (right). Reproduced with permission from ref 25. Copyright 2016 American Association for Advancement of Science.

of their unique potential in biomedical functions and chemical design of novel materials.

AUTHOR INFORMATION

Corresponding Author

*E-mail: stupp@northwestern.edu.

ORCID

Mark P. Hendricks: 0000-0003-1295-9879
Kohei Sato: 0000-0002-8948-8537
Liam C. Palmer: 0000-0003-0804-1168
Samuel I. Stupp: 0000-0002-5491-7442

Notes

The authors declare no competing financial interest.

Biographies

Mark P. Hendricks earned a B.S. in chemistry from Harvey Mudd College in 2010 and a Ph.D. from Columbia University in 2015. He worked under Prof. Jonathan Owen as a graduate student, studying the synthesis of semiconducting nanocrystals. He is currently a postdoctoral fellow in the laboratory of Prof. Samuel Stupp at Northwestern University.

Kohei Sato received a B.S. in chemistry in 2009 from Chiba University. He completed his Ph.D. with Prof. Takuzo Aida at the University of Tokyo in 2014. He is currently a postdoctoral fellow in the laboratory of Prof. Samuel Stupp at Northwestern University.

Liam C. Palmer received a B.S. in chemistry from the University of South Carolina in 1999. He completed his Ph.D. on molecular encapsulation under the supervision of Prof. Julius Rebek, Jr. at The Scripps Research Institute in 2005. He is now a Research Associate Professor in the Department of Chemistry and the Director of Research for the Simpson Querrey Institute for BioNanotechnology at Northwestern University.

Samuel I. Stupp earned a B.S. in chemistry from the University of California at Los Angeles and a Ph.D. in materials science and engineering from Northwestern University in 1977. He was a member of the faculty at Northwestern until 1980 and then spent 18 years at the University of Illinois at Urbana−Champaign before returning to Northwestern in 1999. He is currently Board of Trustees Professor of Materials Science & Engineering, Chemistry, Medicine, and Biomedical Engineering and serves as the director of the Simpson Querrey Institute for BioNanotechnology at Northwestern University. His group's research is focused on the design of new materials through supramolecular chemistry and self-assembly, with an emphasis on functions of interest in advanced medicine and sustainable energy.

ACKNOWLEDGMENTS

The authors are grateful for support of the work discussed herein by grants from Department of Energy (Grant DE-FG02-00ER45810), the DOE-funded Center for Bio-Inspired Energy Science, an Energy Frontier Research Center (Grant DE-SC0000989), the National Institutes of Health (National Institute of Dental and Craniofacial Research 5R01DE015920-9, Bioengineering Research Partnerships 5R01EB003806-09 and 5R01HL116577-02, Center of Cancer Nanotechnology Excellence F5U54CA151880-05, Project Parent Grant P01HL108795-04), and the National Science Foundation (Grant DMR-1508731).

REFERENCES

(1) Jain, R. K.; Gupta, C. M.; Anand, N. Synthesis of Peptidylglycophospholipids, Novel Derivatives of Muramyl-Dipeptide. *Tetrahedron Lett.* **1981**, *22*, 2317−2320.

(2) Thompson, N. L.; Brian, A. A.; McConnell, H. M. Covalent Linkage of a Synthetic Peptide to a Fluorescent Phospholipid and Its Incorporation Into Supported Phospholipid Monolayers. *Biochim. Biophys. Acta, Biomembr.* **1984**, *772*, 10−19.

(3) Berndt, P.; Fields, G. B.; Tirrell, M. Synthetic Lipidation of Peptides and Amino Acids: Monolayer Structure and Properties. *J. Am. Chem. Soc.* **1995**, *117*, 9515−9522.

(4) Carr, C.; Tyler, A. N.; Cohen, J. B. Myristic Acid Is the NH_2-Terminal Blocking Group of the 43-kDa Protein of Torpedo Nicotinic Post-Synaptic Membranes. *FEBS Lett.* **1989**, *243*, 65−69.

(5) Hartgerink, J. D.; Beniash, E.; Stupp, S. I. Self-Assembly and Mineralization of Peptide-Amphiphile Nanofibers. *Science* **2001**, *294*, 1684−1688.

DOI: 10.1021/acs.accounts.7b00297
Acc. Chem. Res. 2017, 50, 2440−2448

(6) Cui, H.; Cheetham, A. G.; Pashuck, E. T.; Stupp, S. I. Amino Acid Sequence in Constitutionally Isomeric Tetrapeptide Amphiphiles Dictates Architecture of One-Dimensional Nanostructures. *J. Am. Chem. Soc.* **2014**, *136*, 12461−12468.
(7) Hartgerink, J. D.; Beniash, E.; Stupp, S. I. Peptide-Amphiphile Nanofibers: a Versatile Scaffold for the Preparation of Self-Assembling Materials. *Proc. Natl. Acad. Sci. U. S. A.* **2002**, *99*, 5133−5138.
(8) Pashuck, E. T.; Cui, H.; Stupp, S. I. Tuning Supramolecular Rigidity of Peptide Fibers Through Molecular Structure. *J. Am. Chem. Soc.* **2010**, *132*, 6041−6046.
(9) Cui, H.; Webber, M. J.; Stupp, S. I. Self-Assembly of Peptide Amphiphiles: From Molecules to Nanostructures to Biomaterials. *Biopolymers* **2010**, *94*, 1−18.
(10) Standley, S. M.; Toft, D. J.; Cheng, H.; Soukasene, S.; Chen, J.; Raja, S. M.; Band, V.; Band, H.; Cryns, V. L.; Stupp, S. I. Induction of Cancer Cell Death by Self-Assembling Nanostructures Incorporating a Cytotoxic Peptide. *Cancer Res.* **2010**, *70*, 3020−3026.
(11) Toft, D. J.; Moyer, T. J.; Standley, S. M.; Ruff, Y.; Ugolkov, A.; Stupp, S. I.; Cryns, V. L. Coassembled Cytotoxic and Pegylated Peptide Amphiphiles Form Filamentous Nanostructures with Potent Antitumor Activity in Models of Breast Cancer. *ACS Nano* **2012**, *6*, 7956−7965.
(12) Moyer, T. J.; Finbloom, J. A.; Chen, F.; Toft, D. J.; Cryns, V. L.; Stupp, S. I. pH and Amphiphilic Structure Direct Supramolecular Behavior in Biofunctional Assemblies. *J. Am. Chem. Soc.* **2014**, *136*, 14746−14752.
(13) Silva, G. A.; Czeisler, C.; Niece, K. L.; Beniash, E.; Harrington, D. A.; Kessler, J. A.; Stupp, S. I. Selective Differentiation of Neural Progenitor Cells by High-Epitope Density Nanofibers. *Science* **2004**, *303*, 1352−1355.
(14) Webber, M. J.; Tongers, J.; Newcomb, C. J.; Marquardt, K.-T.; Bauersachs, J.; Losordo, D. W.; Stupp, S. I. Supramolecular Nanostructures That Mimic VEGF as a Strategy for Ischemic Tissue Repair. *Proc. Natl. Acad. Sci. U. S. A.* **2011**, *108*, 13438−13443.
(15) Capito, R. M.; Azevedo, H. S.; Velichko, Y. S.; Mata, A.; Stupp, S. I. Self-Assembly of Large and Small Molecules Into Hierarchically Ordered Sacs and Membranes. *Science* **2008**, *319*, 1812−1816.
(16) Zha, R. H.; Velichko, Y. S.; Bitton, R.; Stupp, S. I. Molecular Design for Growth of Supramolecular Membranes with Hierarchical Structure. *Soft Matter* **2016**, *12*, 1401−1410.
(17) Zhang, S.; Greenfield, M. A.; Mata, A.; Palmer, L. C.; Bitton, R.; Mantei, J. R.; Aparicio, C.; Olvera de la Cruz, M.; Stupp, S. I. A Self-Assembly Pathway to Aligned Monodomain Gels. *Nat. Mater.* **2010**, *9*, 594−601.
(18) Berns, E. J.; Sur, S.; Pan, L.; Goldberger, J. E.; Suresh, S.; Zhang, S.; Kessler, J. A.; Stupp, S. I. Aligned Neurite Outgrowth and Directed Cell Migration in Self-Assembled Monodomain Gels. *Biomaterials* **2014**, *35*, 185−195.
(19) Korevaar, P. A.; Newcomb, C. J.; Meijer, E. W.; Stupp, S. I. Pathway Selection in Peptide Amphiphile Assembly. *J. Am. Chem. Soc.* **2014**, *136*, 8540−8543.
(20) Tantakitti, F.; Boekhoven, J.; Wang, X.; Kazantsev, R. V.; Yu, T.; Li, J.; Zhuang, E.; Zandi, R.; Ortony, J. H.; Newcomb, C. J.; Palmer, L. C.; Shekhawat, G. S.; Olvera de la Cruz, M.; Schatz, G. C.; Stupp, S. I. Energy Landscapes and Functions of Supramolecular Systems. *Nat. Mater.* **2016**, *15*, 469−476.
(21) Ortony, J. H.; Newcomb, C. J.; Matson, J. B.; Palmer, L. C.; Doan, P. E.; Hoffman, B. M.; Stupp, S. I. Internal Dynamics of a Supramolecular Nanofibre. *Nat. Mater.* **2014**, *13*, 812−816.
(22) da Silva, R. M. P.; van der Zwaag, D.; Albertazzi, L.; Lee, S. S.; Meijer, E. W.; Stupp, S. I. Super-Resolution Microscopy Reveals Structural Diversity in Molecular Exchange Among Peptide Amphiphile Nanofibres. *Nat. Commun.* **2016**, *7*, 11561.
(23) Newcomb, C. J.; Sur, S.; Ortony, J. H.; Lee, O.-S.; Matson, J. B.; Boekhoven, J.; Yu, J. M.; Schatz, G. C.; Stupp, S. I. Cell Death versus Cell Survival Instructed by Supramolecular Cohesion of Nanostructures. *Nat. Commun.* **2014**, *5*, 3321.
(24) Newcomb, C. J.; Sur, S.; Lee, S. S.; Yu, J. M.; Zhou, Y.; Snead, M. L.; Stupp, S. I. Supramolecular Nanofibers Enhance Growth Factor Signaling by Increasing Lipid Raft Mobility. *Nano Lett.* **2016**, *16*, 3042−3050.
(25) Yu, Z.; Tantakitti, F.; Yu, T.; Palmer, L. C.; Schatz, G. C.; Stupp, S. I. Simultaneous Covalent and Noncovalent Hybrid Polymerizations. *Science* **2016**, *351* (6272), 497−502.
(26) Cui, H.; Muraoka, T.; Cheetham, A. G.; Stupp, S. I. Self-Assembly of Giant Peptide Nanobelts. *Nano Lett.* **2009**, *9*, 945−951.
(27) Lee, S. S.; Fyrner, T.; Chen, F.; Álvarez, Z.; Sleep, E.; Chun, D. S.; Weiner, J. A.; Cook, R. W.; Freshman, R. D.; Schallmo, M. S.; Katchko, K. M.; Schneider, A. D.; Smith, J. T.; Yun, C.; Singh, G.; Hashmi, S. Z.; McClendon, M. T.; Yu, Z.; Stock, S. R.; Hsu, W. K.; Hsu, E. L.; Stupp, S. I. Sulfated Glycopeptide Nanostructures for Multipotent Protein Activation. *Nat. Nanotechnol.* **2017**, *12*, 821.
(28) Morgan, C. E.; Dombrowski, A. W.; Pérez, C. M. R.; Bahnson, E. S. M.; Tsihlis, N. D.; Jiang, W.; Jiang, Q.; Vercammen, J. M.; Prakash, V. S.; Pritts, T. A.; Stupp, S. I.; Kibbe, M. R. Tissue-Factor Targeted Peptide Amphiphile Nanofibers as an Injectable Therapy to Control Hemorrhage. *ACS Nano* **2016**, *10*, 899−909.
(29) Rothemund, P. W. K.; Ekani-Nkodo, A.; Papadakis, N.; Kumar, A.; Kuchnir Fygenson, D.; Winfree, E.. Design and Characterization of Programmable DNA Nanotubes. *J. Am. Chem. Soc.* **2004**, *126*, 16344−16352.
(30) Stephanopoulos, N.; Freeman, R.; North, H. A.; Sur, S.; Jeong, S. J.; Tantakitti, F.; Kessler, J. A.; Stupp, S. I. Bioactive DNA-Peptide Nanotubes Enhance the Differentiation of Neural Stem Cells Into Neurons. *Nano Lett.* **2015**, *15*, 603−609.

DOI: 10.1021/acs.accounts.7b00297
Acc. Chem. Res. 2017, 50, 2440−2448